

Counteractions Direct One- or Two-Electron Oxidation of an Al(III) Complex and Al(III)–Oxo Intermediates Activate C–H Bonds

Thomas W. Myers and Louise A. Berben*

Department of Chemistry, University of California, Davis, California 95616, United States

Supporting Information

ABSTRACT: Hydrogen abstraction by aluminum(III)–oxo intermediates via reaction pathways reminiscent of late transition metal chemistry has been observed. Oxidation of $M^+ [(IP^{2-})_2Al]^-$ (IP = iminopyridine, $M = Na, Bu_4N$) yielded $[Na(THF)(DME)][(IP^-)(IP^{2-})Al(OH)]$ (**3**) or $[(IP^-)_2Al(OH)]$ (**4**), via O-atom transfer and subsequent C–H activation or proton abstraction, respectively.

The development of routes for selective functionalization of C–H bonds in hydrocarbon feedstocks remains a significant challenge in modern chemistry.¹ For instance, an important subset of possible transformations is controlled oxidation of C–H bonds. The later first row transition-metal ions, such as manganese, iron, and cobalt, can oxidize C–H bonds via high-valent metal–oxo intermediates. In general, the catalytic cycle starts with oxidation of the transition-metal catalyst to form a reactive metal–oxo intermediate, which then abstracts a hydrogen atom from the substrate. Following this C–H activation, the resulting –OH functionality may “rebound” to the organic substrate to yield an oxidized substrate with C–OH functionality. Significantly, this catalytic cycle involves a redox step in which a higher-valent metal–oxo intermediate results from the reaction of an oxidant with a lower-valent transition-metal precursor.

In principle, cheap and abundant main-group elements such as aluminum are appealing for large-scale applications such as catalysis. However, the reliance on redox processes for transformations involving the metal–oxo group may explain in part why similar chemistry for the generally redox-inactive main-group elements remains far less explored. Recent work has shown that redox-active ligands can engender additional redox activity to transition-metal ions.² In particular, a zirconium complex that can reductively eliminate biphenyl^{3a} and another than can activate O_2 ^{3b} have been reported.

We have previously shown that aluminum(III) complexes with redox-active ligands of the form $(IP^{n-})_2AlX$ [IP = 2,6-bis(1-methylethyl)-*N*-(2-pyridinylmethylene)phenylamine; $n = 0, 1, 2$; X = monodentate ligand] can be isolated in four oxidation states, including an open-shell triplet.⁴ Herein we demonstrate that reactions involving transformations from one redox state of $[(IP^{n-})_2Al]^{m-}$ to another can be effected, that these ligand-based redox processes can be coupled with functionalization of the Al(III) center, and that counteractions strongly influence the reactivity. Facile oxidation of $[(IP^{2-})_2Al]^-$ by pyridine-*N*-oxide (pyO) yields proposed Al(III)–oxo intermediates that react with the C–H bonds in the available solvent or counteractions to give Al(III)–OH complexes. This reaction pathway is more typical of late-transition-metal complexes (Scheme 1).

Scheme 1

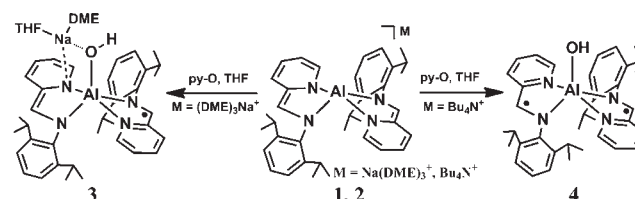


Table 1. Selected Bond Lengths in **3** and **4** (This Work) and in $(IP)AlCl_3$, $(IP^-)_2AlCl$, and $[(IP^{2-})_2Al]^-$ (**1**) (Prior Work) for Comparison

	Al–N _{im}	Al–N _{py}	C _{im} –C _{py}	C _{im} –N _{im}
$(IP)AlCl_3$	2.038(4)	2.084(4)	1.453(7)	1.284(6)
$(IP^-)_2AlCl$	1.915(4)	2.009(15)	1.405(2)	1.354(2)
$[(IP^{2-})_2Al]^-$	1.844(4)	1.873(4)	1.356(6)	1.414(6)
3 (IP^{2-})	1.879(2)	1.956(2)	1.347(3)	1.411(3)
3 (IP^-)	1.948(2)	2.069(2)	1.385(4)	1.349(3)
4 (IP^-)	1.935(3)	2.028(13)	1.396(2)	1.358(2)

A mixture of $[Na(DME)_3][(IP^{2-})_2Al]$ (**1**) (DME = 1,2-dimethoxyethane) with pyO in THF solution was stirred at room temperature for 30 min, during which time the deep-purple color of **1** was replaced by a deep-green color typical of the singly reduced ligand in the $(IP^-)_2AlX$ moiety, which we have previously studied (X = Cl, CF₃SO₃). Single crystals suitable for X-ray diffraction analysis were obtained in 67% yield by cooling a hexane solution of the product at –25 °C for 1 week (Tables S1 and S2 in the Supporting Information). It has been demonstrated that the four bond lengths in Table 1 can aid oxidation state assignments for IP ligands,^{4,5} and the solid-state structure in this case revealed a mixed-valent complex with the formulation $[(IP^-)(IP^{2-})Al(OH)]^-$ in which the IP^{2-} ligand and the hydroxo functional group are bridged by the $[Na(DME)(THF)]^+$ counteraction (Figure 1). The aluminum center is nearly trigonal-bipyramidal ($\tau = 0.851$).⁶ The C_{py}–N_{py} bond length in the IP^{2-} ligand is the only metric that differs from the expected value, and this elongation by 0.04 Å is most likely due to interactions with the Na⁺ ion.

The IR spectrum of **3** displays absorption bands assignable to the OH, C–N_{im}(IP^-), and C–N_{im}(IP^{2-}), 1.5 functional groups (Table S3 and Figure S1). No absorption band definitively

Received: April 26, 2011

Published: July 20, 2011

attributable to a ligand-to-ligand charge-transfer band was observed in the UV–vis–NIR spectrum (Figure S2). The temperature-independent doublet spin state that was predicted on the basis of the molecular structure of **3** was confirmed by susceptibility measurements between 5 and 300 K; the magnetic moment was measured to be $1.83\mu_B$. On the basis of the structure and the IR and NIR spectroscopic data, mixed-valent **3** appears to have a fully localized electronic structure (i.e., Robin and Day class I^7). Cyclic voltammetry (CV) measurements performed on **3** in 0.1 M Bu_4NPF_6 THF solution revealed successive rather than concomitant oxidation and reduction waves for each of the $\text{IP}^{2-/-}$ couples (Figure S3). We attribute this observation to the different electronic environment created at each IP ligand by coordination of Na^+ to one of the pyridine rings.⁸

To observe the oxidation chemistry without the influence of the coordinating Na^+ cation, $[\text{Bu}_4\text{N}][(\text{IP}^{2-})_2\text{Al}]$ (**2**) was prepared from **1** by salt metathesis with Bu_4NI (Figure S4 and Tables S1 and S2). Reaction of **2** with pyO in THF gave complex **4**, which displayed a sharp band in the IR absorption spectrum at 3713 cm^{-1} indicative of the OH functional group. In addition, absorption bands consistent with the IP^- oxidation state of the ligands are apparent (Table S3 and Figure S1).⁹ Single crystals suitable for X-ray diffraction analysis were obtained by cooling a hexane solution of the product at $-25\text{ }^\circ\text{C}$ for 1 week, and the solid-state structure revealed $(\text{IP}^-)_2\text{Al}(\text{OH})$ (**4**) (Figure 1). A symmetry plane bisects the aluminum center in **4**, making the IP^- ligands crystallographically equivalent. Metrics for the bond lengths appeared to agree with the IP^- oxidation state assigned by IR spectroscopy and charge balance, but we could not use these bond distances as definitive evidence for the $(\text{IP}^-)_2\text{Al}(\text{OH})$ formulation. The aluminum center is approximately trigonal-bipyramidal ($\tau = 0.784$). Magnetic susceptibility measurements further supported the formulation of **4** as the triplet biradical $(\text{IP}^-)_2\text{Al}(\text{OH})$; the magnetic moment of $1.5\mu_B$ at 300 K fell to $0.4\mu_B$ at 20 K (Figure S5). A fit to the experimental data using MAGFIT 3.1¹⁰ and a spin Hamiltonian of the form $\hat{H} = -2J\hat{S}_{L(1)} \cdot \hat{S}_{L(2)}$ with $g = 2.0$ supported an electronic model in which two IP^- -based ligand radicals interact antiferromagnetically at low temperature. The energy of the interaction was fit using $J = -370\text{ cm}^{-1}$. This electronic structure is very similar to the triplet biradical structure of $(\text{IP}^-)_2\text{AlCl}$ that was previously reported by us, for which $J = -230\text{ cm}^{-1}$.⁴

It is interesting to note that monomeric aluminum–oxo or –hydroxo complexes are rare. A borane-protected monomeric aluminum–oxo complex¹¹ and a magnesium-capped aluminum–oxo complex¹² have been reported and were obtained by metathesis reactions. Similarly, the hydroxo complexes $\text{LAl}(\text{OH})_2$ and $\text{LAlMe}(\text{OH})$ [$\text{L} = \text{HC}\{(\text{CMe})(2,6\text{-iPrC}_6\text{H}_3\text{N})\}_2$] were obtained by salt metatheses of LAlI_2 and LAlMeCl , respectively, with water/KOH/KH.¹³

It is informative to speculate on the mechanism for the formation of complexes **3** and **4** from **1** and **2**, respectively. When the reaction of **1** with pyO was performed in dry d_8 -THF, the OH IR absorption band in the resulting product was split into two bands at 3711 (OH) and 2707 (OD) cm^{-1} , which represent the products **3** and **3D**, respectively. In a subsequent experiment, complex **1** was initially stirred in d_8 -THF for 24 h. ^1H NMR spectroscopic analysis confirmed that all of the DME in the $[\text{Na}(\text{DME})_3]^+$ counteraction of **1** was replaced by d_8 -THF. After reaction with pyO, IR spectroscopic investigation of the products revealed close to 100% incorporation of D into the OD functional

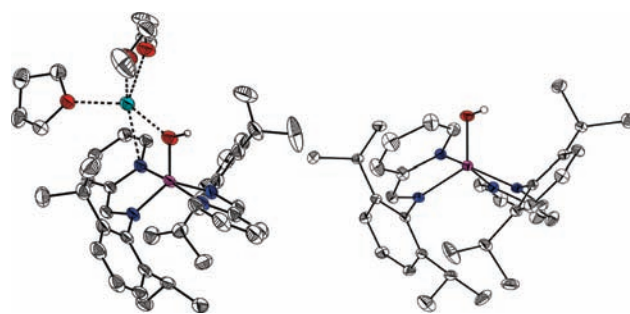


Figure 1. Solid-state structures of $[\text{Na}(\text{DME})(\text{THF})][(\text{IP}^-)(\text{IP}^{2-})\text{Al}(\text{OH})]$ (**3**) and $(\text{IP}^-)_2\text{Al}(\text{OH})$ (**4**).

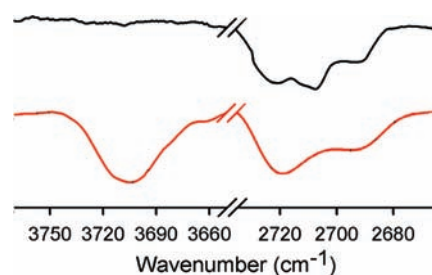


Figure 2. IR absorption spectra for **3** (red) and **3D** (black) in the regions of the OH (3711 cm^{-1}) and OD (2703 cm^{-1}) absorption bands.

group (Figure 2). These observations are consistent with a reaction mechanism in which formation of the Al–O bond and oxidation of **1** are followed by C–H activation of the solvent molecules bound to the Na^+ ion. We observed no evidence for C–H activation of the IP ligand. The reaction of **1** with pyO to form **3** involves only a one-electron oxidation of **1**, although we employed the two-electron oxidant pyO; we postulate that coordination of Na^+ to the py fragment of IP^{2-} stabilizes the $[(\text{IP}^{2-})(\text{IP}^-)\text{Al}(\text{OH})]^-$ moiety toward further oxidation. When the same reaction of **1** with pyO was performed in DME, ether, or dioxane, we again observed formation of the one-electron-oxidized product $[(\text{IP}^{2-})(\text{IP}^-)\text{Al}(\text{OH})]^-$, which was identified by comparison of IR and ^1H NMR spectra with spectra from authentic samples of **3**.

In contrast, the formation of **4** from **2** and pyO involves a two-electron oxidation, and we speculate that in the absence of coordinating Na^+ ion to stabilize IP^{2-} , each of the two IP^{2-} ligands in **2** is oxidized to IP^- as the Al–O bond is formed. Analysis of the reaction mixture by GC–MS and ^1H NMR spectroscopy revealed stoichiometric formation of Bu_3N . This result is consistent with an acid–base process in which proton abstraction from Bu_4N^+ by a putative $[\text{Al}\text{--oxo}]^-$ intermediate to give **4** is followed by elimination of butene from $\text{Bu}_3(\text{Bu}^-)(\text{N}^+)$ to give Bu_3N in a Hoffman-type mechanism.

The reaction pathways and resulting products that we have witnessed are reminiscent of redox transformations associated with transition-metal chemistry.¹ Future endeavors will focus on a more detailed understanding of the mechanisms of these reactions and further development and control of the oxidation chemistry and counteraction effects, aiming toward chemical transformations.

■ ASSOCIATED CONTENT

S Supporting Information. Synthesis and characterization of complexes; X-ray data for **2–4**; CIF files; and results of IR,

UV–vis–NIR, magnetic susceptibility, and CV measurements. This material is available free of charge via the Internet at <http://pubs.acs.org>.

AUTHOR INFORMATION

Corresponding Author

laberben@ucdavis.edu

ACKNOWLEDGMENT

We thank the University of California, Davis for funding and Profs. J. Shaw and A. Moulé for use of GC–MS and UV–vis–NIR instruments, respectively.

REFERENCES

- (1) Gunay, A.; Theopold, K. H. *Chem. Rev.* **2010**, *110*, 1060.
- (2) For example, see: (a) Lu, C. C.; DeBeer George, S.; Weyhermüller, T.; Bill, E.; Bothe, E.; Wieghardt, K. *Angew. Chem., Int. Ed.* **2008**, *47*, 1. (b) Smith, A. L.; Clapp, L. A.; Hardcastle, K. I.; Soper, J. D. *Polyhedron* **2010**, *29*, 164. (c) Sylvester, K. T.; Chirik, P. J. *J. Am. Chem. Soc.* **2009**, *131*, 8772.
- (3) (a) Hameline, M. R.; Heyduk, A. H. *J. Am. Chem. Soc.* **2006**, *128*, 8410. (b) Stanciu, C.; Jones, M. E.; Fanwick, P. E.; Abu-Omar, M. M. *J. Am. Chem. Soc.* **2007**, *129*, 12400.
- (4) Myers, T. W.; Kazem, N.; Stoll, S.; Britt, R. D.; Shanmugam, M.; Berben, L. A. *J. Am. Chem. Soc.* **2011**, *133*, 8662.
- (5) Lu, C. C.; Bill, E.; Weyhermüller, T.; Bothe, E.; Wieghardt, K. *J. Am. Chem. Soc.* **2008**, *130*, 3181.
- (6) Addison, A. W.; Rao, T. N.; Van Rijn, J. J.; Verschoor, G. C. *J. Chem. Soc., Dalton Trans.* **1984**, 1349.
- (7) Robin, M. B.; Day, P. *Adv. Inorg. Chem. Radiochem.* **1967**, *10*, 247.
- (8) Alternatively, the spacing between successive redox waves could be due to rearrangement of **3** following initial electron transfer.
- (9) For previously reported imine spectra, see: Kincaid, K.; Gerlach, C. P.; Giesbrecht, G. R.; Hagadorn, J. R.; Whitener, G. R.; Shafir, A.; Arnold, J. *Organometallics* **1999**, *18*, 5360.
- (10) Schmitt, E. A. Ph.D. Thesis, University of Illinois at Urbana-Champaign, Urbana, IL, 1995.
- (11) Neculai, D.; Roesky, H. W.; Neculai, A. M.; Magull, J.; Walfort, B.; Stalke, D. *Angew. Chem., Int. Ed.* **2002**, *41*, 4294.
- (12) Nembenna, S.; Roesky, H. W.; Mandal, S. K.; Oswald, R. B.; Pal, A.; Herbst-Immer, R.; Noltemeyer, M.; Schmidt, H. G. *J. Am. Chem. Soc.* **2006**, *128*, 13056.
- (13) (a) Bai, G.; Peng, Y.; Roesky, H. W.; Li, J.; Schmidt, H. G.; Noltemeyer, M. *Angew. Chem., Int. Ed.* **2003**, *42*, 1433. (b) Bai, G.; Singh, S.; Roesky, H. W.; Noltemeyer, M.; Schmidt, H. G. *J. Am. Chem. Soc.* **2005**, *127*, 3449.